

Original Article

Location and dynamic changes of inflammation, fibrosis, and expression levels of related genes in SiO₂-induced pulmonary fibrosis in rats *in vivo*

Zhao-qiang Zhang¹, Bo Shao¹, Gui-zhi Han¹, Gen-yi Liu¹, Chun-zhi Zhang¹, and Li Lin^{1*}

¹ Department of Public Health, Jining Medical University, 45 Jianshe South Road, Jining city, Shandong Province 272113, China

Abstract: Silicosis is a serious occupational disease characterized by pulmonary fibrosis, and its mechanism and progression have not been fully elucidated yet. In this study, silicosis models of rat were established by a one-time dusting method, and the rats were sacrificed after 30, 60, and 120 days (herein referred to as the 30, 60, and 120 days groups, respectively). The rats without dust exposure were used as the control. The lungs were removed to observe pathological changes using hematoxylin and eosin and Masson's trichrome staining and transmission electron microscopy, and the degree of collagen type I and III deposition in the lung was evaluated by enzyme-linked immunosorbent assay. The levels of malondialdehyde and superoxide dismutase were measured by spectrophotometry, and the expression levels of fibrosis-related genes (transforming growth factor beta 1, type I collagen, type III collagen) were assessed by real-time quantitative polymerase chain reaction. The results suggested that the rats in the model groups exhibited obvious collagen fibrosis and that the severity of the lung injury increased as the time after exposure to SiO₂ increased. There was a significant response to lung inflammation in the model rats, especially in the 30 days group. The degree of lipid peroxidation in bronchoalveolar lavage fluid cells and lung tissues in experiment group rats significantly increased. Among the three fibrosis-related genes, transforming growth factor beta 1 was elevated in both bronchoalveolar lavage fluid cells and lung tissues of the experiment group rats, while collagen type I and III were only elevated in lung tissues. Hence, we concluded that as silicosis progressed, inflammation, fibrosis, and the expression of fibrosis-related genes showed different time-dependent changes and that a number of causal relationships existed among them. (DOI: 10.1293/tox.2019-0024; J Toxicol Pathol 2019; 32: 253–260)

Key words: silicosis, inflammation, fibrosis, fibrosis-related gene

Introduction

Silicosis is an irreversible and incurable lung disease caused by the inhalation of dust containing crystalline silica particles¹. It is epidemic worldwide^{2,3}, and developing countries have typically been associated with a high incidence of it⁴. To date, no 100% therapeutic approaches have been presented for silicosis, and the average survival time of patients is 3–5 years⁵. Importantly, this disease seriously threatens the health and safety of workers.

The pathogenesis of silicosis has not been fully elucidated. Studies have shown that silicosis is a pathological condition in which lungs become scarred due to excess deposition of extracellular matrix (ECM)^{6,7}. The ECM is mainly composed of plasma proteins secreted by myofibro-

blasts, which represent an activated state of fibroblasts^{8,9}. During fibrosis, plasma and extracellular proteins are cross-linked by enzymes to eventually form insoluble nodules¹⁰. A study showed that supernatants from SiO₂-treated macrophages can induce activation of fibroblasts and increase the collagen content of ECM⁶. However, the types and time of distribution of fibrosis, expression of the related genes and their location in the lungs, as well as the relationship between SiO₂-induced inflammation and the abovementioned fibrosis-related genes have remained elusive.

In this experiment, a rat model of silicosis was established to observe the inflammation and fibrosis of lung tissue, the oxidation state of bronchoalveolar lavage fluid (BALF) cells and lung tissue, and the expression of genes related to fibrosis in BALF cells and lung tissue. This study also aimed to analyze the time-dependent changes of the effects of inflammation and expression of fibrosis-related genes on collagen fibrosis during silicosis and to explore the association between inflammation, fibrosis, and expression of related genes. This study may provide new therapeutic insight for prevention and treatment of silicosis.

Received: 26 March 2019, Accepted: 18 June 2019

Published online in J-STAGE: 10 August 2019

*Corresponding author: L Lin (e-mail: linli6711@sina.com)

©2019 The Japanese Society of Toxicologic Pathology

This is an open-access article distributed under the terms of the Creative Commons Attribution Non-Commercial No Derivatives

(by-nc-nd) License. (CC-BY-NC-ND 4.0: <https://creativecommons.org/licenses/by-nc-nd/4.0/>).



Materials and Methods

Chemicals

Silica particles that had a crystalline form and were smaller than 5 μm in diameter were obtained from the Chinese Center for Disease Control and Prevention (Beijing, China). The distribution of the sizes was as follows: 50% <1.0 μm , 85% <2.0 μm , 98% <5.0 μm . Physiological saline (Shandong Lukang Pharmaceutical Factory Inc., Shandong, China) was used as the vehicle for silica particles (Fig. 1).

Animals and grouping

This experiment was conducted in compliance with the *Guidelines for Animal Experimentation at the Institute of Occupational Health and Environmental Medicine of Jining Medical University*. The animal protocol was designed to minimize pain or discomfort in the animals. Male specific-pathogen-free (SPF) Wistar rats that were 6 weeks old were provided by the Laboratory Animal Center of Jining Medical University (Jining, China). The rats were housed in a climate-controlled room at a temperature of $20 \pm 3^\circ\text{C}$ and humidity of $60 \pm 5\%$ with a 12 h dark-light cycle. The rats were fed with standard food and water. After acclimation over one week, the rats were divided into 30, 60, and 120 days experimental groups and 1 control group ($n=10$ in each group). Before intratracheal instillation, the rats were anesthetized with 3.0% isoflurane for 15 min using a face mask with an inhalation anesthesia system. As soon as anesthesia was accomplished, a standard bulb-tipped gavage needle was inserted into the epiglottis via the mouth using an operating otoscope with a speculum. One milliliter of SiO_2 suspension (100 mg/mL) was injected into the trachea with the syringe driver^{11,12}. Then the rats were shaken clockwise for 3 min to ensure that the silica particles completely entered

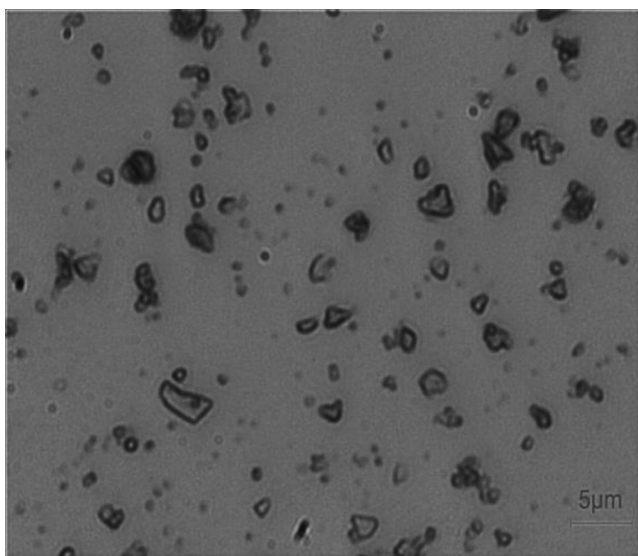


Fig. 1. Representative microscopic view of silica dust (bar =5 μm). Most of the particles were less than 5 μm in diameter.

the lungs. The rats were then sacrificed by exsanguination under light isoflurane anesthesia after 30, 60, and 120 days. The control group rats were treated in the same way except that 1 mL of physiological saline was injected into the lung through the trachea, and the rats were sacrificed after 120 days.

Tissue sampling and histopathology

Left lung tissue (<0.3 mm^3) was removed, fixed in 4% paraformaldehyde, and embedded in paraffin. It was then sliced into thin sections (5 μm) using standard techniques. The sections were stained with hematoxylin and eosin (HE) to visualize histopathological changes such as inflammatory infiltrates. Collagen deposition on the sections was observed using images of Masson's trichrome staining, in which collagen was stained blue. At the same time, lung tissue (<0.1 mm^3) was fixed in 1.0% glutaraldehyde and postfixed in 1% osmium tetroxide solution (pH 7.4) for 2 h, and then it was processed into thin sections. The ultrastructure of the lung was observed under transmission electron microscope (TEM; JEOL Ltd., Tokyo, Japan).

Analysis of collagen types I and III by enzyme-linked immunosorbent assay

Lung tissues were homogenized in buffer and centrifuged (at $1,000 \times g$ for 10 min) to obtain liquid supernatants. Double-antibody sandwich enzyme-linked immunosorbent assays (ELISAs) were used to assess the levels of collagen type I and III in supernatants according to the manufacturer's instructions (Shanghai Enzyme-linked Biotechnology Co., Ltd., Shanghai, China). Optical density at 450 nm was measured using an ELISA reader (Thermo Fisher Scientific Inc., Waltham, MA, USA), and the antigen level (in ng/mL) was calculated. The relative contents of collagen type I and III (in mg/g) in each sample were normalized by the protein concentration (in g/mL) of the corresponding supernatant, which was determined using a BCA Kit (Nanjing Jiancheng Bioengineering Institute, Nanjing, China).

Lipid peroxidation analysis of BALF cells and lung tissue

Cold sterile saline (2 mL) was injected into the right lung alveoli via the trachea five times. The lavage fluid was combined into a plastic tube and centrifuged at $1,200 \times g$ for 10 min. The BALF cells were stored at -80°C until analysis. The contents of superoxide dismutase (SOD), malondialdehyde (MDA), and protein of the BALF cells and lung tissues were measured by spectrophotometry using commercial kits (Nanjing Jiancheng Bioengineering Institute).

mRNA quantification with real-time quantitative PCR

The total RNA of BALF cells and lung tissues was extracted using Trizol reagent (Takara Bio Inc., Kusatsu, Japan). The relative contents of three fibrosis-related genes, including transforming growth factor beta 1 (TGF- β 1), type I collagen, and type III collagen were assessed using real-time quantitative polymerase chain reaction (RT-qPCR).

The three genes were synthesized using a PrimeScript RT reagent kit (Takara Bio Inc.) and RT-qPCR Kit (Takara Bio Inc.) with SYBR Green (Thermo Fisher Scientific Inc.) on an RT-qPCR Detection System (Bio-Rad Laboratories Inc., Hercules, CA, USA) according to the manufacturer's instructions. The expression of the three mentioned genes in each sample was normalized by the expression level of glyceraldehyde-3-phosphate dehydrogenase (GAPDH). The primer sequences used for RT-qPCR were as follows: TGF- β 1, 5'-GGCACCATCCATGACATGAACCG-3' and 5'-GCCGTACAC AGCAGTTCTTCTCTG-3'; type I collagen, 5'-TGTTGGTCCTGCTGGCAAGAATG-3' and 5'-GTCACC TTGTTGCGCTGTCTCAC-3'; type III collagen, 5'-GAC ACGCTGGTGCTCAAGGAC -3' and 5'- GTTCGCTG AAGGACCTCGTTG-3'; and GAPDH, 5'-GACATGCCG CCTGGAGAAACG-3' and 5'-AGCCCAGGATGCCCTGT-3'.

Statistical analysis

The data were analyzed by using the SPSS 17.0 software (SPSS Inc., Chicago, IL, USA) and were expressed as the mean \pm standard deviation (SD). One-way ANOVA followed by the *LSD* test was performed on the results. Difference were considered statistically significant when $P < 0.05$.

Results

Macroscopic analysis

The rats in the control group grew normally without any discomfort or other abnormalities. Rats in the 30 days group showed mild hair loss and mania. Rats in the 60 days group showed more hair loss and slow movement. Rats in the 120 days group had severe hair loss, dull hair, lethargy, and slow movement.

In regard to macroscopic findings, white spots and pulmonary hemorrhage were seen on the surfaces of the lungs in the dust-exposed groups: In the control group, the lungs were soft and elastic, and the surfaces were lustrous. In the 30 days group, obvious edema of lungs was noted, accompanied by a small amount of dark red hemorrhagic areas on the surface. In the 60 days group, the elasticity of the lungs was significantly reduced, and the color of their surfaces was gray-white with obvious scattered protrusions. In the 120 days group, the elasticity of the lungs was poor. There were many spots of congestion on their surfaces, as well as many millet-sized gray-white nodules.

Histopathological analyses

The pathologic images of lung tissues stained with HE showed that higher numbers of infiltrating cells appeared in the alveoli in each experimental group compared with that in the control group. In addition, spindle-shaped fibroblasts, destroyed alveolar structures, and thickening of the interstitial lung could be found as well. The changes were more obvious as time after exposure to the dust increased (Fig. 2). In the images of Masson's trichrome staining, there was obvious blue staining in the experimental groups compared with that in the control group, indicating the proliferation

of collagen fiber. The proliferation was more obvious as the time after exposure to the dust increased (Fig. 3).

Electron microscopic observation

Compared with the control group, there was a significant inflammatory reaction in the 30 days group for macrophages and other infiltrating cells, and slight fibrosis was found. The inflammation in the 60 days group was remarkably relieved compared with that in the 30 days group, while the fibrosis was further aggravated, and the morphology of alveolar type II epithelial (ATE II) cells changed. In the 120 days group, inflammation was further alleviated, fibrosis was more severe, and there was no normal lung tissue in the field of view; the tissue was replaced by hyperplastic and fused fibers (Fig. 4).

Deposition of collagen type I and III in the lung

Regarding the collagen deposition levels, silica dust increased the relative contents of collagen type I and III. For collagen type I, the effect became significant in all experimental groups compared with the control group ($P < 0.05$), while for collagen type III, the effect became obvious in the 60 and 120 days groups ($P < 0.05$; Table 1).

Lipid peroxidation level in BALF cells and lung tissues

Compared with the control group, the MDA content in the three experimental groups increased ($P < 0.05$), especially in the 30 days group, however, the activity of SOD decreased compared with that in the control group ($P < 0.05$; Table 2).

mRNA Expression in BALF cells and lung tissues

Compared with the control group, the expression of TGF- β 1 markedly increased in both BALF cells and lung tissues ($P < 0.05$). Additionally, the expression levels of collagen types I and III were increased only in lung tissues ($P < 0.05$; Table 3).

Discussion

Collagen is the main structural protein in ECM, constituting the main framework of lung tissue^{13, 14}, and its content should be maintained at a reasonable level, as abnormal levels may damage cells¹⁵. A previous study revealed that abnormal accumulation of ECM in lung tissues plays a pivotal role in pulmonary fibrosis¹⁶. Silicosis is a lung disease caused by the inhalation of crystalline silica dust¹⁷. The pathological results in the present study showed that collagen fiber hyperplasia and intrapulmonary thickening occurred in all silicosis model rats. The conditions were more serious as the time after exposure to dust increased. These findings were confirmed by electron microscopic observation as well.

Silicosis is a progressive process, depending on the amount of collagen synthesis controlled by related genes. The contents of protein of collagen type I and III notably in-

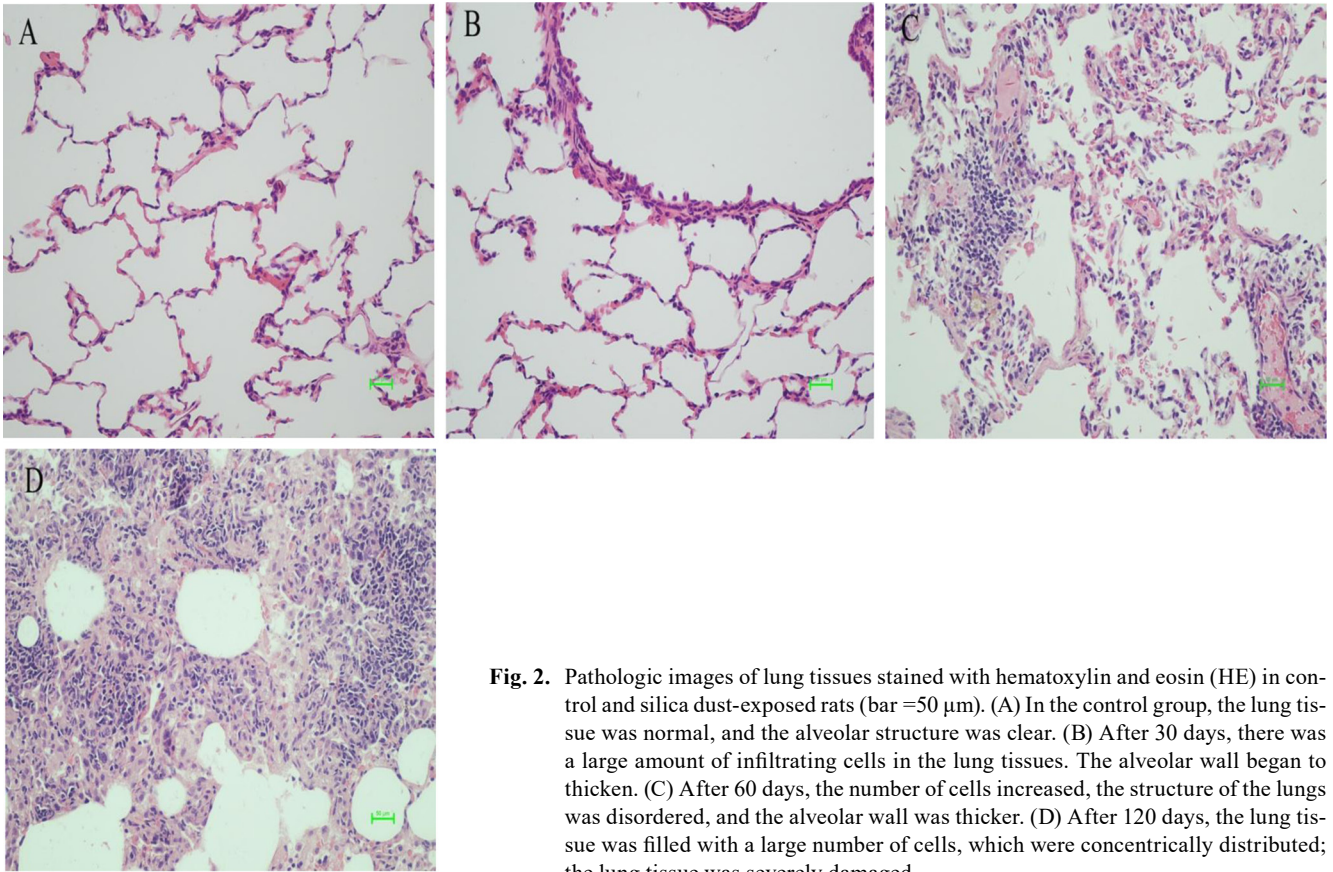


Fig. 2. Pathologic images of lung tissues stained with hematoxylin and eosin (HE) in control and silica dust-exposed rats (bar =50 μ m). (A) In the control group, the lung tissue was normal, and the alveolar structure was clear. (B) After 30 days, there was a large amount of infiltrating cells in the lung tissues. The alveolar wall began to thicken. (C) After 60 days, the number of cells increased, the structure of the lungs was disordered, and the alveolar wall was thicker. (D) After 120 days, the lung tissue was filled with a large number of cells, which were concentrically distributed; the lung tissue was severely damaged.

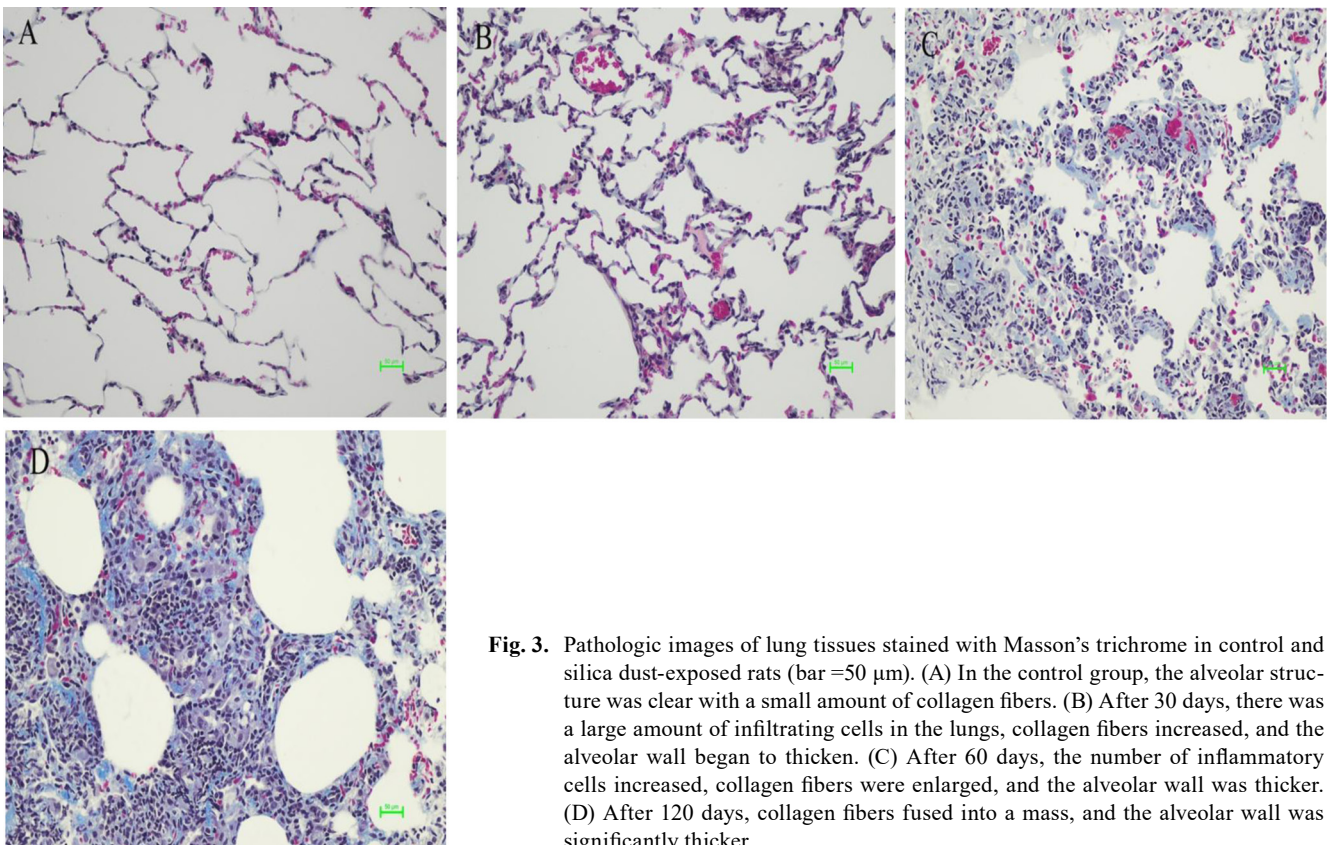


Fig. 3. Pathologic images of lung tissues stained with Masson's trichrome in control and silica dust-exposed rats (bar =50 μ m). (A) In the control group, the alveolar structure was clear with a small amount of collagen fibers. (B) After 30 days, there was a large amount of infiltrating cells in the lungs, collagen fibers increased, and the alveolar wall began to thicken. (C) After 60 days, the number of inflammatory cells increased, collagen fibers were enlarged, and the alveolar wall was thicker. (D) After 120 days, collagen fibers fused into a mass, and the alveolar wall was significantly thicker.

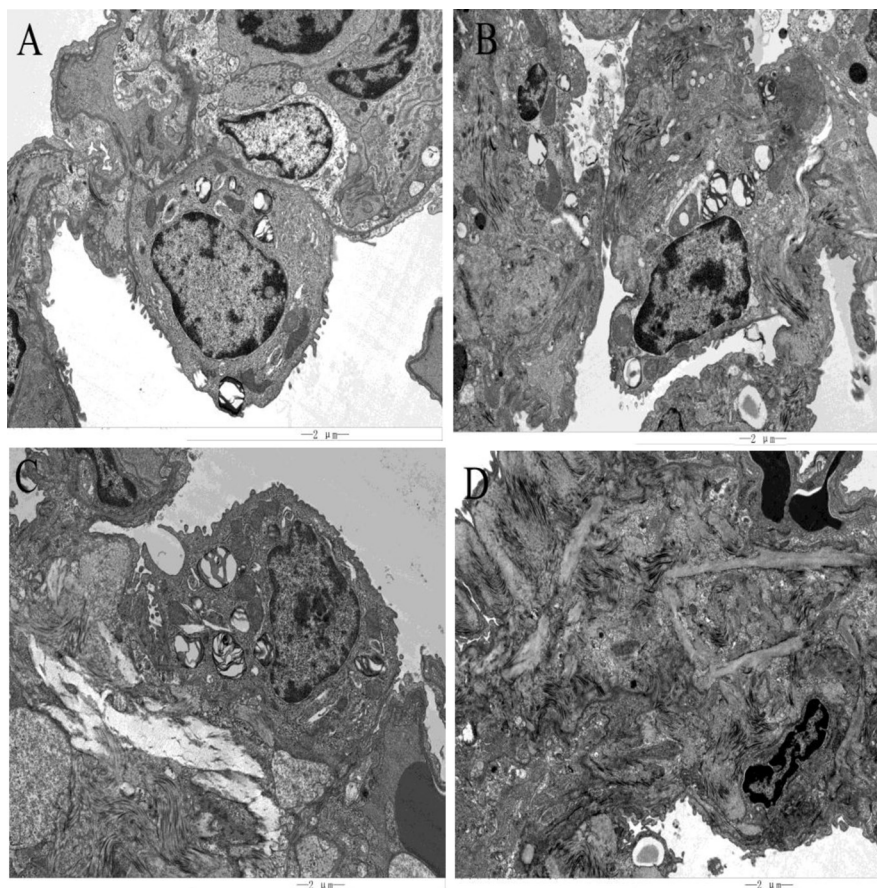


Fig. 4. Transmission electron microscope (TEM) images of lung tissues in control and silica dust-exposed rats (bar = 2 μ m). (A) In the control group, the lung tissue was clearly structured, showing alveolar type I cells and alveolar type II cells. The alveolar type I cells were elongated; the alveolar type II cells were elliptical, showing lamellar bodies with large nuclei and villi on the membrane. (B) After 30 days, alveolar type II cells with a large nucleus, a few lamellar bodies in the cells, and lodging and falling off of villi on the membrane could be observed. There was a small amount of fibrosis around alveolar type II cells. There were several exfoliated cells and tissues around the interstitial lung, and the inflammatory reaction was severe. (C) After 60 days, alveolar type II cells with a large nucleus and blurred nuclear membrane could be observed. There were a large number of lamellar bodies in the cells. In the left and lower parts of alveolar type II cells, there was obvious fibroplasia. There were exfoliated cells and tissues around the interstitial lung, and inflammation was decreased compared with that in the 30 days group. (D) After 120 days, all fibers in the field of view were hyperplastic fibers that had been fused. At the lower right of the section, the remaining alveolar type II cells, which were partially fibrotic, were observed. There were a small number of detached cells and tissues around the interstitial lung, and the inflammatory response was further alleviated.

Table 1. Levels of Collagen Type I and Collagen Type III in the Lung of Rats

Group	Collagen type I (mg/g)	Collagen type III (mg/g)
Control	1.12 \pm 0.23	2.22 \pm 0.48
30 days	2.08 \pm 0.22*	2.73 \pm 0.53
60 days	3.29 \pm 0.18*	4.33 \pm 0.54*
120 days	3.77 \pm 0.14*	6.23 \pm 0.52*

Values are mean \pm SD; n=10. * P <0.05 compared with control group.

creased in pulmonary fibrosis, and they are often known as indexes of pulmonary fibrosis^{18, 19}. This feature appeared in the silicosis model rats in this study too. During the course of silicosis fibrosis, the location and dynamic changes of the expressed fibrosis-related genes have shown significant in-

fluences on the occurrence, progression, and prognosis of silicosis fibrosis. This is the reason why BALF cells and lung tissues were selected as subjects in this study. In summary, the following conclusions can be drawn from our results:

1. The locations of the expressed fibrosis-related genes were different in the lungs. TGF- β 1 was expressed in both BALF cells and lung tissues, while collagen type I and III were expressed only in lung tissues. The BALF cells contained many kinds of cells, and pulmonary macrophages were the predominant cells^{20, 21}. Previous researchers have reported TGF- β 1, secreted by SiO₂-activated macrophages, playing a key role in the development of silicosis^{22, 23}. The location of activated pulmonary macrophages is related to the distribution of toxins, protecting the body against their harmful effects²⁴. In this study, the majority of the silica dust was inhaled into alveoli, and a small amount of dust

Table 2. Lipid Peroxidation of Bronchoalveolar Lavage Fluid (BALF) Cells and Lung Tissue in Rats

Group	BALF cells		Lung tissue	
	MDA (nmol/mg·pro)	SOD (U/mg·pro)	MDA (nmol/mg·pro)	SOD (U/mg·pro)
Control	2.10 ± 0.21	63.35 ± 5.20	2.00 ± 0.28	63.61 ± 4.96
30 days	6.02 ± 0.18*	33.07 ± 4.78*	4.11 ± 0.21*	40.10 ± 5.03*
60 days	5.44 ± 0.22*	38.42 ± 5.21*	3.65 ± 0.16*	44.53 ± 4.57*
120 days	5.21 ± 0.20*	42.94 ± 4.99*	3.29 ± 0.22*	46.21 ± 4.66*

Values are mean ± SD; n=10. **P*<0.05 compared with control group. MDA: malondialdehyde, SOD: superoxide dismutase.

Table 3. Relative Contents of the Three Fibrosis-related Genes mRNA of Bronchoalveolar Lavage Fluid (BALF) Cells and Lung Tissue in Rats

Group	TGF-β1 mRNA		Type I collagen mRNA		Type III collagen mRNA	
	BALF cells	Lung tissue	BALF cells	Lung tissue	BALF cells	Lung tissue
Control	1.01 ± 0.58	1.20 ± 0.63	0.98 ± 0.38	1.12 ± 0.36	0.80 ± 0.37	0.96 ± 0.42
30 days	10.90 ± 1.06*	7.56 ± 0.67*	1.26 ± 0.36	1.56 ± 0.38*	0.76 ± 0.35	1.22 ± 0.36
60 days	6.03 ± 0.71*	5.31 ± 0.49*	1.31 ± 0.42	2.56 ± 0.42*	1.01 ± 0.40	2.37 ± 0.53*
120 days	3.50 ± 0.89*	2.01 ± 0.57	1.28 ± 0.41	2.26 ± 0.35*	1.20 ± 0.56	1.76 ± 0.44*

Values are mean ± SD; n=10. **P*<0.05 compared with control group.

adhered to the alveolar wall or entered into the interstitium. Macrophages in those locations could take in silica dust, and this could stimulate them to secrete TGF-β1 there.

The expression levels of collagen type I and III are related to myofibroblasts, which are generally taken into account as the major effect cells of fibrosis⁷. Pedigree tracking experiments showed that a variety of cells in the interstitial lung can differentiate into myofibroblasts^{5, 25}. In idiopathic pulmonary fibrosis (IPF), the main source of myofibroblasts is fibrocyte-derived myofibroblasts, which comprise up to 50% of their content²⁶. Another source of myofibroblasts is alveolar type II epithelial (ATE II) cells^{7, 27}. Fibroblasts and ATE II cells are both located in fixed positions, justifying why collagen type I and III were expressed in lung tissues rather than in BALF cells.

2. The expression levels of the three related genes in the experimental groups increased, but their peak values appeared in different stages. In this study, the fact that the peak expression of collagen type I and III occurred after the peak expression of TGF-β1 indicated a possible causal relationship between these proteins: the total level of TGF-β1 secreted by BALF cells and lung tissues activated the expression of collagen type I and III, which was supported by the finding of previous studies^{22, 28}. This study also showed a different pattern of expression for collagen type I and III. Type I collagen showed a significant expression after 30 days, reached its peak expression level after 60 days, and then decreased; type III collagen showed no significant increase after 30 days, reached its peak expression level after 60 days, and then decreased. The above results indicated that type I collagen is more sensitive compared with type III collagen during fibrosis, and this was found to be consistent with the findings presented by Van Hoozen *et al.*²⁹, in contrast to those reported by Lai *et al.*³⁰.

3. The present study also showed a negative synergistic change between inflammation and the expression levels

of the abovementioned three genes, and inflammation was involved in the development of silicosis. In the early stage of the silicosis model, pulmonary inflammation was severe, and TGF-β1 expression was significant, while silicosis fibrosis was mild. In a later stage, inflammation decreased, and TGF-β1 expression was attenuated, whereas silicosis fibrosis was aggravated. The expression of collagen type I and III also changed in a manner similar to TGF-β1. Inflammation can generate reactive oxygen species (ROS), which was revealed by an increase in MDA and a decrease in SOD in this study. In general, ROS are considered to be executing mediators of a series of damaging effects induced by inflammation. It has been reported that inflammation could activate macrophages to generate TGF-β1 through the ROS pathway^{31, 32}. It has also been reported that TGF-β1 acted on pulmonary interstitial fibroblasts and activated the expression of collagen type I and III^{33, 34}. Similarly, when inflammation is reduced, the level of ROS is decreased, the expression of fibrosis-related genes is reduced, and newly formed collagen fibers are decreased. Under physiological conditions, the body's collagen maintains a dynamic balance between production and degradation, while in the process of pulmonary fibrosis, the production of collagen fiber increased, but degradation pathway are inhibited, therefore collagen fibers are deposited in the lung³⁵. The degree of silicosis fibrosis depends on the accumulation of newly formed collagen in different periods. Therefore, we hypothesized that an anti-inflammatory may help slow down the onset of fibrosis and reduce the risk of silicosis, and this point of view was also supported by Carneiro *et al.*³⁶.

Disclosure of Potential Conflicts of Interest: The authors have no conflicts of interest to declare.

Acknowledgements: This research was supported by the Natural Science Foundation of Shandong Province (Grant

No. ZR2017MH085) and National Natural Science Foundation Cultivation Project of Jining Medical University (Grant No. JYP201719).

References

- Li C, Du S, Lu Y, Lu X, Liu F, Chen Y, Weng D, and Chen J. Blocking the 4–1BB pathway ameliorates crystalline silica-induced lung inflammation and fibrosis in mice. *Theranostics*. **6**: 2052–2067. 2016. [Medline] [CrossRef]
- Fan C, Graff P, Vihlborg P, Bryngelsson IL, and Andersson L. Silica exposure increases the risk of stroke but not myocardial infarction—A retrospective cohort study. *PLoS One*. **13**: e0192840. 2018. [Medline] [CrossRef]
- Martínez C, Prieto A, García L, Quero A, González S, and Casan P. Silicosis: a disease with an active present. *Arch Bronconeumol*. **46**: 97–100. 2010. [Medline] [CrossRef]
- Chen S, Cui G, Peng C, Lavin MF, Sun X, Zhang E, Yang Y, Guan Y, Du Z, and Shao H. Transplantation of adipose-derived mesenchymal stem cells attenuates pulmonary fibrosis of silicosis via anti-inflammatory and anti-apoptosis effects in rats. *Stem Cell Res Ther*. **9**: 110. 2018. [Medline] [CrossRef]
- Habel DM, and Hogaboam CM. Heterogeneity of fibroblasts and myofibroblasts in pulmonary fibrosis. *Curr Pathobiol Rep*. **5**: 101–110. 2017. [Medline] [CrossRef]
- Lian X, Chen X, Sun J, An G, Li X, Wang Y, Niu P, Zhu Z, and Tian L. MicroRNA-29b inhibits supernatants from silica-treated macrophages from inducing extracellular matrix synthesis in lung fibroblasts. *Toxicol Res (Camb)*. **6**: 878–888. 2017. [Medline] [CrossRef]
- Li J, Yao W, Hou JY, Zhang L, Bao L, Chen HT, Wang D, Yue ZZ, Li YP, Zhang M, Yu XH, Zhang JH, Qu YQ, and Hao CF. The role of fibrocyte in the pathogenesis of silicosis. *Biomed Environ Sci*. **31**: 311–316. 2018. [Medline]
- Liu Y, Xu H, Geng Y, Xu D, Zhang L, Yang Y, Wei Z, Zhang B, Li S, Gao X, Wang R, Zhang X, Brann D, and Yang F. Dibutylryl-cAMP attenuates pulmonary fibrosis by blocking myofibroblast differentiation via PKA/CREB/CBP signaling in rats with silicosis. *Respir Res*. **18**: 38. 2017. [Medline] [CrossRef]
- Peng HB, Wang RX, Deng HJ, Wang YH, Tang JD, Cao FY, and Wang JH. Protective effects of oleanolic acid on oxidative stress and the expression of cytokines and collagen by the AKT/NF- κ B pathway in silicotic rats. *Mol Med Rep*. **15**: 3121–3128. 2017. [Medline] [CrossRef]
- Kim YM, Chung SI, and Lee SY. Roles of plasma proteins in the formation of silicotic nodules in rats. *Toxicol Lett*. **158**: 1–9. 2005. [Medline] [CrossRef]
- Liu N, Xue L, Guan Y, Li QZ, Cao FY, Pang SL, and Guan WJ. Expression of peroxiredoxins and pulmonary surfactant protein a induced by silica in rat lung tissue. *Biomed Environ Sci*. **29**: 584–588. 2016. [Medline]
- Liu H, Cheng Y, Yang J, Wang W, Fang S, Zhang W, Han B, Zhou Z, Yao H, Chao J, and Liao H. BBC3 in macrophages promoted pulmonary fibrosis development through inducing autophagy during silicosis. *Cell Death Dis*. **8**: e2657. 2017. [Medline] [CrossRef]
- Li XD, Wu YP, Chen SH, Liang YC, Lin TT, Lin T, Wei Y, Xue XY, Zheng QS, and Xu N. Fasudil inhibits actin polymerization and collagen synthesis and induces apoptosis in human urethral scar fibroblasts via the Rho/ROCK pathway. *Drug Des Devel Ther*. **12**: 2707–2713. 2018. [Medline] [CrossRef]
- Tang M, Ding S, Min X, Jiao Y, Li L, Li H, and Zhou C. Collagen films with stabilized liquid crystalline phases and concerns on osteoblast behaviors. *Mater Sci Eng C*. **58**: 977–985. 2016. [Medline] [CrossRef]
- Harrington DJ. Bacterial collagenases and collagen-degrading enzymes and their potential role in human disease. *Infect Immun*. **64**: 1885–1891. 1996. [Medline]
- Kim KK, Kugler MC, Wolters PJ, Robillard L, Galvez MG, Brumwell AN, Sheppard D, and Chapman HA. Alveolar epithelial cell mesenchymal transition develops in vivo during pulmonary fibrosis and is regulated by the extracellular matrix. *Proc Natl Acad Sci USA*. **103**: 13180–13185. 2006. [Medline] [CrossRef]
- Minelli G, Zona A, Cavariani F, Comba P, and Pasetto R. Silicosis mortality in Italy: temporal trends 1990–2012 and spatial patterns 2000–2012. *Ann Ist Super Sanita*. **53**: 275–282. 2017. [Medline]
- Guo W, Shan B, Klingsberg RC, Qin X, and Lasky JA. Abrogation of TGF- β 1-induced fibroblast-myofibroblast differentiation by histone deacetylase inhibition. *Am J Physiol Lung Cell Mol Physiol*. **297**: L864–L870. 2009. [Medline] [CrossRef]
- Kage H, and Borok Z. EMT and interstitial lung disease: a mysterious relationship. *Curr Opin Pulm Med*. **18**: 517–523. 2012. [Medline]
- Sellamuthu R, Umbricht C, Roberts JR, Young SH, Richardson D, McKinney W, Chen BT, Li S, Kashon M, and Joseph P. Molecular mechanisms of pulmonary response progression in crystalline silica exposed rats. *Inhal Toxicol*. **29**: 53–64. 2017. [Medline] [CrossRef]
- Sharma SK, Pande JN, Verma K, and Guleria JS. Bronchoalveolar lavage fluid (BALF) analysis in interstitial lung diseases—a 7-year experience. *Indian J Chest Dis Allied Sci*. **31**: 187–196. 1989. [Medline]
- Sun Y, Yang F, Yan J, Li Q, Wei Z, Feng H, Wang R, Zhang L, and Zhang X. New anti-fibrotic mechanisms of n-acetylseryl-aspartyl-lysyl-proline in silicon dioxide-induced silicosis. *Life Sci*. **87**: 232–239. 2010. [Medline] [CrossRef]
- Xu H, Yang F, Sun Y, Yuan Y, Cheng H, Wei Z, Li S, Cheng T, Brann D, and Wang R. A new antifibrotic target of AcSDKP: inhibition of myofibroblast differentiation in rat lung with silicosis. *PLoS One*. **7**: e40301. 2012. [Medline] [CrossRef]
- Rodero MP, Poupel L, Loyher PL, Hamon P, Licata F, Pessel C, Hume DA, Combadière C, and Boissonnas A. Immune surveillance of the lung by migrating tissue monocytes. *eLife*. **4**: e07847. 2015. [Medline] [CrossRef]
- Sakai N, and Tager AM. Fibrosis of two: Epithelial cell-fibroblast interactions in pulmonary fibrosis. *Biochim Biophys Acta*. **1832**: 911–921. 2013. [Medline] [CrossRef]
- Gomperts BN, and Strieter RM. Fibrocytes in lung disease. *J Leukoc Biol*. **82**: 449–456. 2007. [Medline] [CrossRef]
- Serrano-Mollar A, Gay-Jordi G, Guillamat-Prats R, Closa D, Hernandez-Gonzalez F, Marin P, Burgos F, Martorell J, Sánchez M, Arguis P, Soy D, Bayas JM, Ramirez J, Tetley TD, Molins L, de la Bellacasa JP, Rodríguez-Villar C, Rovira I, Fiblà JJ, Xaubet A; Pneumocyte Study Group. Safety

- and tolerability of alveolar type II cell transplantation in idiopathic pulmonary fibrosis. *Chest*. **150**: 533–543. 2016. [[Medline](#)] [[CrossRef](#)]
28. Deng CW, Zhang XX, Lin JH, Huang LF, Qu YL, and Bai C. Association between genetic variants of transforming growth factor- β 1 and susceptibility of pneumoconiosis: a meta-analysis. *Chin Med J (Engl)*. **130**: 357–364. 2017. [[Medline](#)] [[CrossRef](#)]
 29. Van Hoozen BE, Grimmer KL, Marelich GP, Armstrong LC, and Last JA. Early phase collagen synthesis in lungs of rats exposed to bleomycin. *Toxicology*. **147**: 1–13. 2000. [[Medline](#)] [[CrossRef](#)]
 30. Lai CK, Wallace WD, and Fishbein MC. Histopathology of pulmonary fibrotic disorders. *Semin Respir Crit Care Med*. **27**: 613–622. 2006. [[Medline](#)] [[CrossRef](#)]
 31. Latella G. Redox imbalance in intestinal fibrosis: beware of the TGF β -1, ROS, and Nrf2 connection. *Dig Dis Sci*. **63**: 312–320. 2018. [[Medline](#)] [[CrossRef](#)]
 32. Ahamed J, and Laurence J. Role of platelet-derived transforming growth factor- β 1 and reactive oxygen species in radiation-induced organ fibrosis. *Antioxid Redox Signal*. **27**: 977–988. 2017. [[Medline](#)] [[CrossRef](#)]
 33. Dong Z, Zhao X, Tai W, Lei W, Wang Y, Li Z, and Zhang T. IL-27 attenuates the TGF- β 1-induced proliferation, differentiation and collagen synthesis in lung fibroblasts. *Life Sci*. **146**: 24–33. 2016. [[Medline](#)] [[CrossRef](#)]
 34. Ezzoukhry Z, Henriot E, Piquet L, Boyé K, Bioulac-Sage P, Balabaud C, Couchy G, Zucman-Rossi J, Moreau V, and Saltel F. TGF- β 1 promotes linear invadosome formation in hepatocellular carcinoma cells, through DDR1 up-regulation and collagen I cross-linking. *Eur J Cell Biol*. **95**: 503–512. 2016. [[Medline](#)] [[CrossRef](#)]
 35. McKleroy W, Lee TH, and Atabai K. Always cleave up your mess: targeting collagen degradation to treat tissue fibrosis. *Am J Physiol Lung Cell Mol Physiol*. **304**: L709–L721. 2013. [[Medline](#)] [[CrossRef](#)]
 36. Carneiro PJ, Clevelario AL, Padilha GA, Silva JD, Kitoko JZ, Olsen PC, Capelozzi VL, Rocco PR, and Cruz FF. Bosutinib therapy ameliorates lung inflammation and fibrosis in experimental silicosis. *Front Physiol*. **8**: 159. 2017. [[Medline](#)] [[CrossRef](#)]